

AIRBORNE OBSERVATIONS OF ICE ACCRETION AND AIRCRAFT PERFORMANCE IN ARTIFICIAL AND NATURAL SUPERCOOLED ICE CLOUDS ON DORNIER 228- AND 328 AIRCRAFT

Franz Schröder*, Dieter Welte**, and Thomas Hauf***

*Inst. für Physik der Atmosphäre, DLR, D-82234 Wessling, Germany

**Dornier Luftfahrt GmbH, D-82230 Wessling, Germany

*** Inst. für Meteorologie und Klimatologie, Universität Hannover, Germany

Keywords: *aircraft icing, supercooled large drops, airborne observations*

Abstract

Results from two airborne experiments investigating aircraft icing, aircraft performance and cloud microphysics associated with supercooled large drops (SLD) are presented. Dornier-*Luftfahrt* performed in-flight tests, where external surfaces of a DO-328 turboprop aircraft were exposed to artificially generated SLD with 180 μm mean volume diameter (MVD). High liquid water content (LWC) up to 0.65 g m^{-3} caused substantial ice accretion behind boot-protected regions of the wings. Visual cues associated with SLD are described. Limitations for flights in severe icing conditions and exiting procedures have been derived.

DLR performed several research flights

within natural icing conditions on a Do-228 aircraft equipped with cloud microphysical- and icing documentation instrumentation. Specified weather-forecasts helped to find atmospheric regions that were characterized by at least moderate icing conditions and temporarily by the occurrence of SLD. Two cases with severe icing and ice accretion rates exceeding 3 mm min^{-1} , temporarily associated with SLD, have been met. SLD did not dominate, but significantly contributed to LWC during icing incidents. Back-running ice has been observed in the presence of SLDs. Heavy icing was experienced in stratiform clouds with embedded convection, average LWC below 0.3 g m^{-3} and within a -10 to -7 $^{\circ}\text{C}$ temperature interval.



Figure 1: Dornier ice tanker (DIT) and following test aircraft (TAC) equipped with OAP-1D sensing probe, ice accretion cylinders and video camera

1. Introduction

Aircraft icing represents a severe problem to aviation. World-wide discussion focuses on the role of supercooled large drops (SLD) with diameters of 50- to 500 μm . These drops are suspected to be the cause of several fatal accidents, e.g. the ATR-72 crash in Roselawn, Il, USA, in 1994. The FAR/JAR-25 icing certification frames (Appendix C) are suspected not to cover all possible atmospheric conditions that can turn out hazardous, especially for smaller sized aircraft with limited ceiling, turboprop engines, pneumatic de-icing boots and manually actuated control surfaces. Neither precise definitions of which meteorological situations necessarily lead to SLD-formation, nor approved standard instrumentation which allows safe- and accurate detection of supercooled liquid water distribution are available as operational standards.

After the fatal accident of the ATR-72 in 1994, the FAA requested manufacturers of regional aircraft with a pneumatic boots de-icing system and hand-powered flight controls to investigate the behavior of the aircraft type during flight in freezing drizzle/rain conditions. Specific instructions for pilots to recognize and exit SLD icing conditions, including maneuvers, use of autopilot, flaps and speed, were requested. Dornier started an investigation of ice accretion behind the protected area on the wing of DO-328 type aircraft during flight in artificial SLD conditions. As a second step, the handling quality and performance characteristics of the DO-328 aircraft with

simulated ice accretion shapes on the wing surfaces were tested in flight.

Within the European Icing Certification Experiment (EURICE) in 1997 (Hauf 1998, Hauf and Schröder 1998), the Department of Atmospheric Physics at DLR performed several research flights within natural icing conditions on a DO-228 type aircraft. The purpose of the study was specifically the search for SLD, favoring meteorological conditions and documentation of related aircraft icing. Present activities aim for the physical understanding of SLD generating processes and evaluation of forecast procedures.

2. Dornier Test Aircraft - Artificial ice clouds

The Dornier 228 Ice Tanker (DIT, Fig. 1) is equipped with a spray array mounted behind the tail. The spray array has an octagonal shape, 1,60 m diameter and can be equipped with changing types of up to 61 spray nozzles. A 1000 liters tank, a pump and a metering unit provide the nozzles with water with a pressure of up to 85 bars. The speed for icing tests shall be chosen between 150 to around 170 knots calibrated airspeed (KCAS). For a given nozzle type, the desired LWC is generated by varying the water pressure and the distance away from the spray array. The ambient air temperature for the test shall be chosen with the altitude. The artificial ice cloud has been characterized by means of a PMS-OAP-1D instrument mounted below the wing of the Dornier 328-100 test aircraft (TAC, Fig.1).

Instruments	Parameter	Range
6 Icing cylinders	Ice accretion	Outer wing
1 Metering plate	Ice accretion	Upper outer wing
Video-monitoring	Ice accretion	Upper/lower wing
Johnson-Williams-Probe	LWC	< 40-50 μm
PMS-OAP1DC	SLD _{DIT} -size spectra	18- 600 μm
P,T, RH meteorological sensors		

Table1 : Icing documentation and microphysical instrumentation on DO-328 test aircraft

AIRBORNE OBSERVATIONS OF ICE ACCRETION AND AIRCRAFT PERFORMANCE IN ARTIFICIAL AND NATURAL SUPERCOOLED ICE CLOUDS ON DORNIER 228- AND 328 AIRCRAFT

The Dornier 328-100 is a regional transport aircraft for 33 passengers, driven by 2 turboprop engines. It is a high-wing, T-tail aircraft configuration. The leading edges of the wing and tail are ice-protected by pneumatic boots. The TAC is equipped with a conventional flight test data recording system. Special equipment for icing tests is listed in Table 1 and shown in Fig. 1. The scope of initial tests was to validate the spray cloud for the meteorological conditions for clouds with SLD as recommended by the FAA (Ashley et al. 1995). The DIT was thus equipped with spray nozzles generating droplet spectra as given in Fig. 2. Several in-flight calibration tests have been performed with change of water pressure, distance and speed.

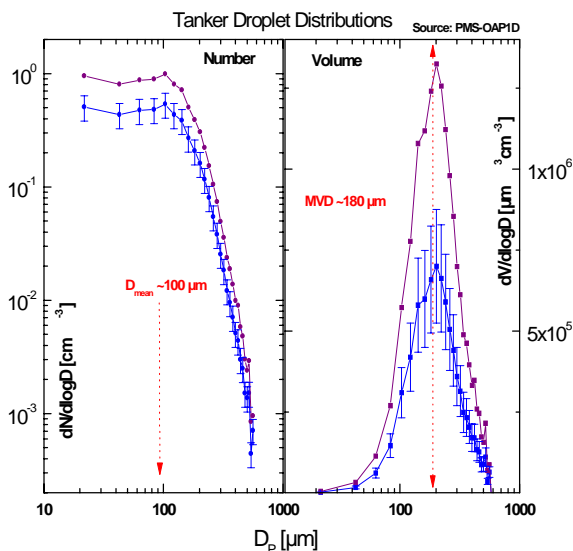


Figure 2: “Cloud“ Drop Number- and Volume Distribution generated by the DIT. Error bars mark systematic uncertainties in OAP-concentration values; the 2 different spectra illustrate a typical variability range during exposure.

SLD conditions were met best with 20 bars water pressure, a distance between the spray array and the TAC of around 40 m, and a speed of 180 knots true airspeed (KTAS). From the Johnson-Williams-probe signal, together with icing cylinder

information, a permanent LWC of 0.4-.65 g m⁻³ was derived.

3. Ice accretion in artificial ice clouds

The flight tests were performed in winter 1996, 11 flights behind the DIT with a total of 5,5 hours inside the spray cloud. Seven flights took place in simulated freezing drizzle conditions with totally 3.5 hours endurance in cloud. Two flight conditions have been chosen: (1): *high* angle of attack (AOA) of the wing, which results in a high droplet impingement intensity on the *lower* wing surface and (2): *low* AOA, resulting in a high droplet impingement intensity on the *upper* wing surface.

3.1 Ice accretion at high AOA, landing flaps up, 160 KCAS, T= -5°C, SLD_{DIT}

The boots kept the leading edge area clear of ice. Between the boots cycles the common residual ice with an average height of a quarter of an inch was visible. Ice accretion behind the active area of the boots occurred characterized by a spanwise narrow ridge. During the exposure time of 25 minutes the ridge built to a height of between 10 and 15 mm and a width of 15 to 20 mm with the spanwise extent of 2 m which corresponds to the width of the artificial cloud.

After that time the ridge broke away in several pieces of different length. Obviously, the small gap on the wing surface between the aft end of the boots and the metal sheet was the nucleus for the ice accretion.

Some dispersed ice accretion appeared on the lower surface of the wing back as far as 30% of the wing chord. The height was some millimeter up to 5 mm with some ice knobs of about 10 mm height. Figure 3 shows the ice accretion on the upper and lower wing surface after 20 minutes exposure to the SLD.



Figure 3: Ice accretion on upper and lower wing side behind the boot protected region, high AOA

3.2 Ice accretion at low AOA, landing flaps 12°, 170 KCAS, T= -5°C, SLD_{DIT}

The boots kept the leading edge area clear of ice. Between the cycles the common residual ice was visible. Two spanwise ridges of ice accreted on the upper surface from 9% to 11% wing chord. The upstream ridge builds up on the aft end of the boots (non-active area 25 mm width) and the downstream ridge on the gap between the boots and the metal sheet. During the exposure time of 25 minutes the two ridges grew together into a single ridge of 15 mm maximum height and 25 to 35 mm width.

No ice accreted on the metal sheet behind the boot.

During the SLD encounter parts of the ridge repeatedly broken away, preferably during the cycle of the boot. It is estimated, that at any time during exposure the ridge covered less than 70% of the span, sometimes only 30% or less. On the lower wing surface only a dispersed ice roughness of less than a few millimeters thickness combined with some ice knobs of less than 10 mm height were visible. Fig. 4 shows typical pictures of the ice accretion on the upper surface before and after boot inflation, after more than 25 minutes SLD exposure.



Figure 4: Ice accretion on upper wing side before- and after boot activation, low AOA

3.3 Visual cues for the pilot

The 1 inch wide, unheated edge of the front window adjacent to the frames is covered with granular dispersed, translucent or opaque ice crystals (Fig. 4b). These patterns occurred within a few minutes after exposure to SLD. Droplets were splashing on impact with the windshield. In contrast, droplets which are covered by the FAR certification envelope are so small, that they are usually below the threshold of visual detectability.

Fig. 8.1: Visual Cue, Freezing Drizzle/Rain, Left and Right Front Window
T 30570



exposure 3 minutes

Fig. 4b: Ice accretion at the cockpit window frame of the TAC after a few minutes exposure to the SLD_{DIT}

The propeller spinner was fully covered with ice during SLD-exposure. The ice coverage was translucent with granular dispersed surface. The ice accretion on the lower surface depends very much on the AOA. At low AOA, 20 minutes exposure to SLD, small lumps or knobs of ice are dispersed on the lower surface behind the boots, not much conspicuous from the pilot cockpit view. At high AOA, and after 20 minutes exposure to SLD, an extensive coverage of the lower surface behind the boots was observed by the pilot, extending

downstream as far as 50% of the local wing chord.

3.4 Aerodynamic performance degradation due to SLD ice accretion

As a next step, artificial ridges have been mounted onto the aircraft's wings. Those are of triangular cross section, 15 mm height, 25 mm wide, with front edge orientation perpendicular to the base. The surface of the artificial ridge was covered by sand grain with roughness of 1 mm height. The ridge itself with constant cross section was made of wood and attached to the upper surface of the nosebox, along the full span at a chordwise position corresponding to the rear end of the de-icing boots, which is around 9% of the local wing chord. For flight-safety reasons, the ridge was build up step by step during repeated flights.

The objective was to investigate the stall speed (V_{s1g}) and the stall characteristics compared to the undisturbed aircraft performance. To define V_{s1g} , the maximum lift was determined for each of 4 possible landing flap settings. The loss of maximum lift caused by the artificial ridges compared to the undisturbed wing profile turned out 52% with landing flaps up and 37.5% with flaps in the landing position. This results in an increase of the stalling speed by 44% and 27%, respectively. The handling quality characteristics did not change significantly and were regarded as tolerable. Effective stall warning was still present. At high speeds up to V_{MO} (= 270 KCAS) no effects on the handling qualities were observed.

Based on these findings, visual cues for the pilots to recognize SLD icing conditions, a procedure for exiting hazardous SLD environments, including maneuvers, use of autopilot, flaps and speed, have been defined and introduced into the Do328-100 Aircraft Flight Manual (AFM), Effectivity 23rd September. 97.

Instrument	Parameter	Detection Range
PMS- OAP-2DC	drop size	20-750 μm
PMS- FSSP-100 ER	drop size	6-98 μm
PMS- FSSP- 300	Aerosol/drop size	0.35-20 μm
Johnson-Williams-Probe	LWC	< 40-50 μm
TSI-3760A CNCs Aerosol Sensors	Aerosol number	> 0.005, 0.014 μm
CEV Icing Cylinder	ice accretion	0-30 mm
Meteorological sensors	T, p, RH	
Video-monitoring	ice accretion	leading edge, lower wing side

Table 2: Cloud microphysical and icing documentation instrumentation on DLR-DO-228 research aircraft

4. Icing in natural supercooled clouds

Not many experimental studies exist on freezing drizzle and related aircraft icing (e.g. Cober et al. 1995, 1996, Politovitch 1989, Sand et al. 1984, Strapp et al. 1996). During March 1997, a DLR research aircraft type DO-228 (2 engine turboprop, same type as the DIT in Fig. 1) has been equipped with a set of icing documentation- and cloud microphysical instrumentation listed in Table 2. The cloud water content (water and ice, CWC) has been evaluated by a Johnson-Williams-probe (which measures liquid water content (Jowi-LWC) up to 40-50 μm drop diameter) together with the cloud element volume distributions derived from the optical spectrometers. Ice accretion on wings and an icing cylinder (CEV, 4 cm diameter) has been monitored by video cameras. Six flight missions within the EURICE program have been performed over Southern Germany, North of the Alps. The general weather situation from mid March to mid April was governed by north-westerly flow transporting cold humid air masses into Central Europe. We focussed on weather conditions suspected to favor the occurrence of SLD, namely low level stratiform clouds, preferably containing convective cells. Considerable icing has been experienced in 5 cases, two cases with moderate to severe icing incidences are reported here.

4.1 Mission on March 15th

During 2 time sequences (entitled SLD1 and SLD2) of about 6 min each the aircraft

penetrated supercooled stratiform cloud layers of about 400 m vertical depth. Sampling was mostly conducted in the cloud top region at 3-3.1 km and 3.3-3.4 km at temperatures of -8 to -9 $^{\circ}\text{C}$ and around -11 $^{\circ}\text{C}$, respectively. Strongest aircraft icing up to 3.5 mm min^{-1} has been experienced during SLD1, where the Jowi-LWC typically ranged between 0.25-0.3 g m^{-3} and the CWC temporarily peaked to more than the double value on spatial scales of about 100- 300 m (Fig. 5). The photo in Figure 6 has been taken short past exit from the SLD1-sequence.

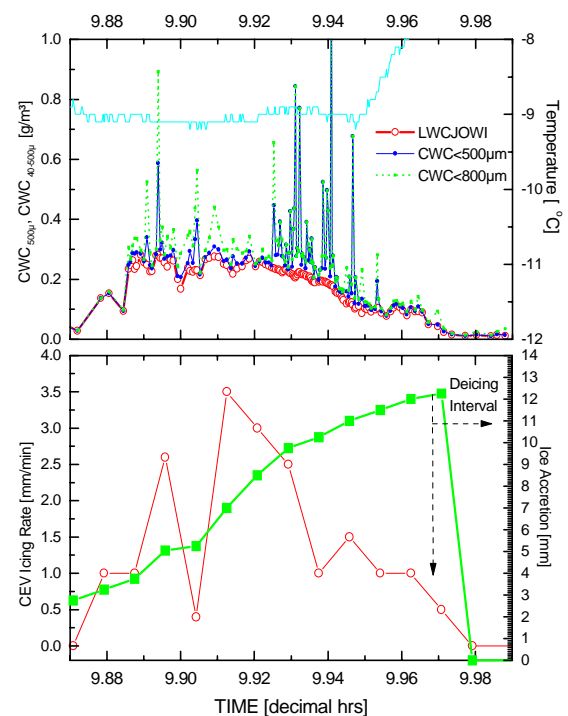


Fig. 5: Jowi-LWC, CWC, and ambient temperature (above), ice accretion on the CEV and icing rate (below) during SLD1, March 15th

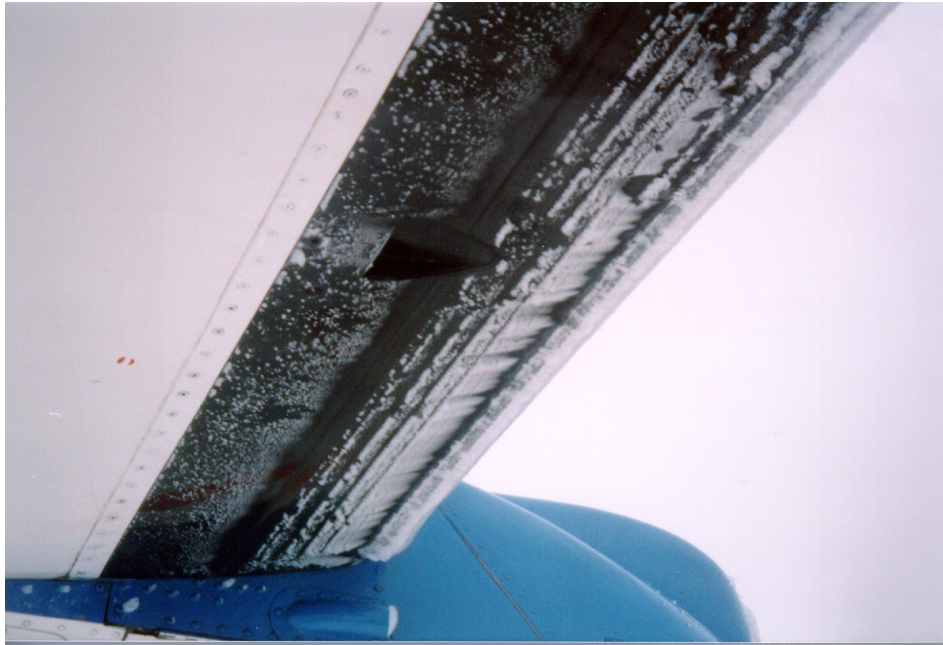


Fig. 6: Ice accretion (SLD1) on the leading edge and behind the boot-protected region below the wing of the DO-228 aircraft

Besides more than 12 mm ice accretion on the leading edge and the CEV, a considerable amount of ice is observed down to 30 cm behind the protected regions below the wing. The number size- and volume spectra of the cloud elements during SLD1 (Fig. 7) show bimodal structure with about $50\text{-}80\text{ cm}^{-3}$ cloud mode drops of about $D_{\text{mean}}=20\text{ }\mu\text{m}$ and (in average) at least 3 orders of magnitude less SLDs with $D_{\text{mean}} \sim 150\text{ }\mu\text{m}$.

In average, the SLD-mode carries not more than about 20% of the supercooled LWC up to cloud element diameters about $500\text{ }\mu\text{m}$. From OAP-2DC image population analysis (comparable to Fig. 10) we expect larger particles ($>500\text{ }\mu\text{m}$) to be fully glaciated (graupel ice) and not contributing to the aircraft icing. In average over SLD1 even the MVD stays below $30\text{ }\mu\text{m}$ and is covered by the FAR/JAR25 Appendix C frame. However this does not necessarily hold for peak events (Fig. 5) and the related SLD-spectra (Fig. 7, thin lines): During SLD1 the MVD temporarily exceeds $80\text{ }\mu\text{m}$ while the cloud drop mode exhibits much less variability in LWC and spectral position. Other flight missions (e.g. on March 24th) with additional radar information strongly support that convective cells within stratified cloud layers generate such cloud spectra with exceptional many SLD.

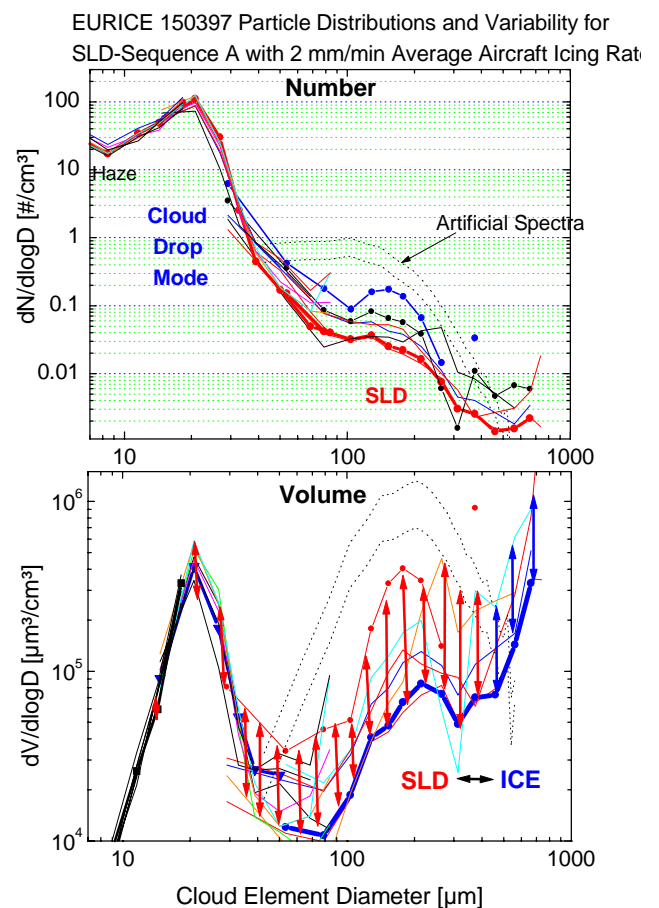


Fig. 7 (left): Composite cloud element number (above) spectra (FSSP300, FSSP100, OAP2DC) and volume distributions during SLD1, March 15th. Bold lines indicate a 3-min average. Arrows mark the short scale variability. For comparison (dotted lines): artificial tanker spectra of the DIT

Fig. 8 illustrates that during SLD2 at $T \approx -11^\circ\text{C}$ comparable peaking SLD were much less frequent, if not absent, which was also evident from the OAP2DC particle spectra (not shown). Although high icing rates up to 2.5 mm min^{-1} occurred, the wing surface behind the boot protected region was not significantly affected.

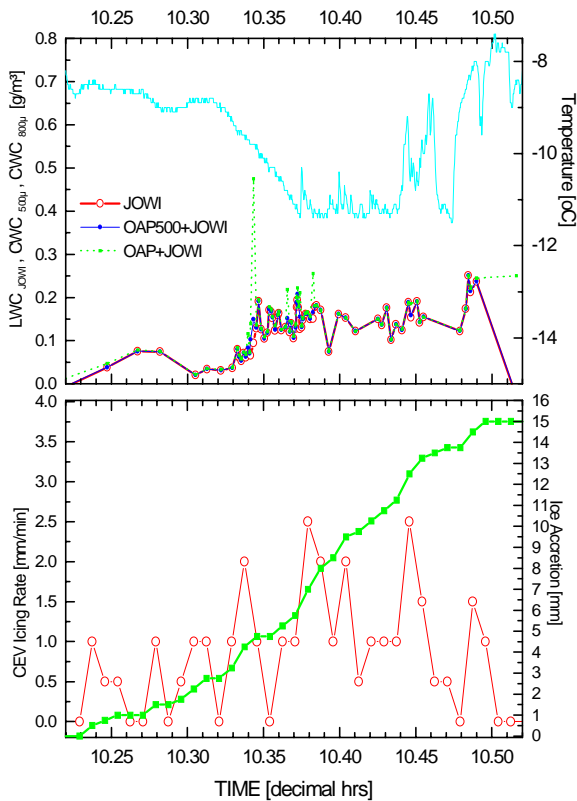


Fig. 8: Jowi-LWC, CWC, and ambient temperature (above), ice accretion onto the CEV and icing rate (below) during SLD2, March 15th

4.2 Mission on March 24th

The flight mission of March 24th focussed on more systematical cloud sampling, again inside stratiform clouds with approximate base/tops between about 1.8- and 3.2 km. Weather-radar was utilized in search for embedded convection and drizzle precipitation. The DO-228 transected comparable (but not necessary the same) convective cells on 5 levels (A-E, Fig. 9) and experienced icing rates up to 3 mm min^{-1} with increasing tendency towards cloud top. A cumulative ice accretion of almost 4 cm onto the CEV was reached. The deicing boots on the wing leading edge were activated twice before the aircraft was forced to exit the upper cloud region at about 12.8 decimal hours (Fig. 9). By

that time the engine thrust level was already increased from about 45% to about 80% to keep a true air speed of 80 m s^{-1} .

Fig. 10 summarizes the most important cloud parameters in a statistical manner. On each level A-E at least several minutes data during cloud penetration have been evaluated with respect to icing rate-, Jowi-LWC-, and CWC-variability. Clearly evident is a correlation of maximum icing rates and *average* LWC (connected by lines in Fig. 10) which directly relates the icing rates to supercooled water bound to the cloud drop mode (around $15 \mu\text{m}$). Both parameters also increase toward cloud top. $D_{\text{mean}} \sim 15 \mu\text{m}$ and cloud drop concentrations clearly exceeded 100 cm^{-3} (not shown), pointing to significantly more but smaller cloud mode drops compared to March 15th.

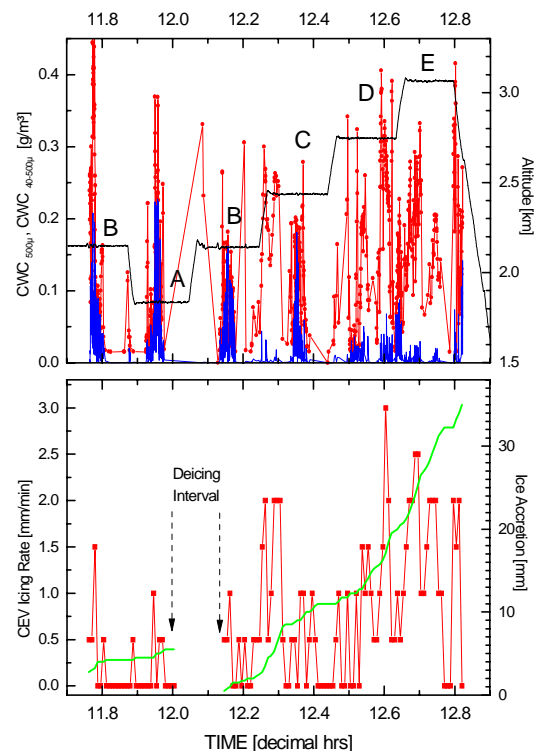


Fig. 9: Integral CWC and CWC $>40 \mu\text{m}$ and altitude (above), ice accretion onto the CEV and icing rate (below), during 1 h cloud sampling on 5 different levels A-E, March 24th.

The fact that a comparably high amount of CWC gets accumulated inside *larger* cloud elements ($>42 \mu\text{m}$) towards cloud base does not seem to enhance the icing rate (Fig. 10). As also Fig. 11 illustrates, the dominating CWC-fraction

**AIRBORNE OBSERVATIONS OF ICE ACCRETION AND AIRCRAFT PERFORMANCE
IN ARTIFICIAL- AND NATURAL SUPERCOOLED ICE CLOUDS ON DORNIER 228- AND 328
AIRCRAFT**

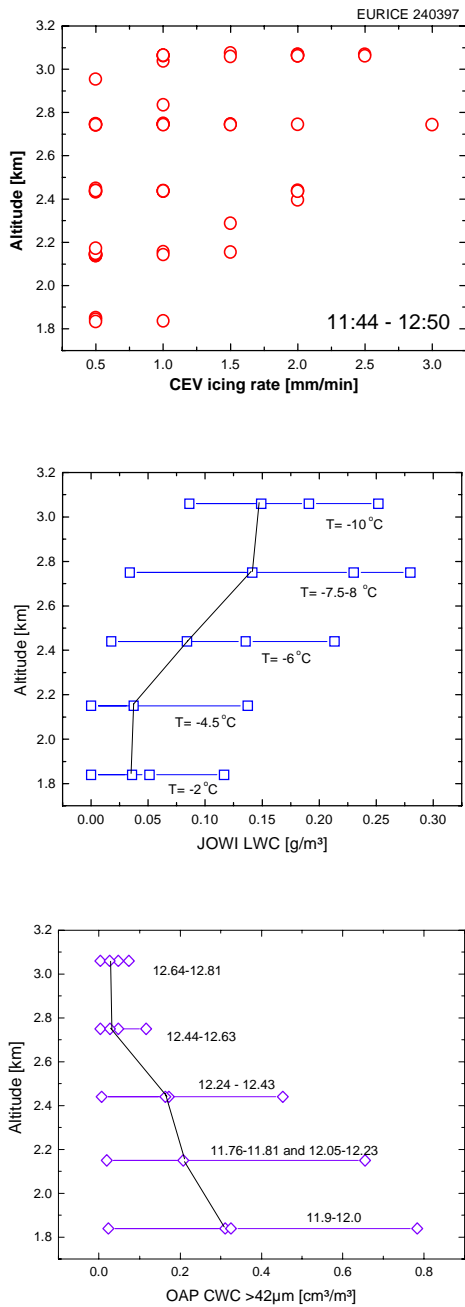


Fig. 10: Above: Altitude-dependent icing rates observed on March 24th. Middle: 25-, 75-, and 90% percentiles and averages (connected by vertical lines) of the Jowi-LWC during the sequences A-E, as well as level temperatures. Below: As middle panel but for OAP-derived CWC > 46 µm. Additionally: time intervals of averaging for level A-E.

is bound to huge (>500 µm) cloud elements near cloud base.

By their irregular shapes they are identified as graupel ice crystals and possibly don't significantly contribute to the observed icing. On the other hand, the cloud element images

near cloud top (~50-200 µm in diameter, Fig. 11, above) imply that those particles could indeed be liquid SLDs.

We admit that although the average LWC-values on March 24th exceeded those measured on March 15th, the icing rates did not do necessarily. Icing behind the protected boot areas was much weaker, if at all present.

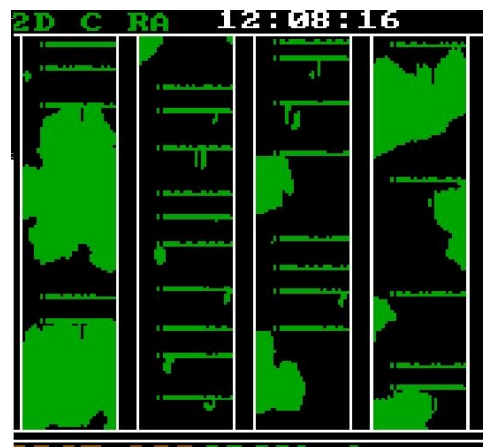
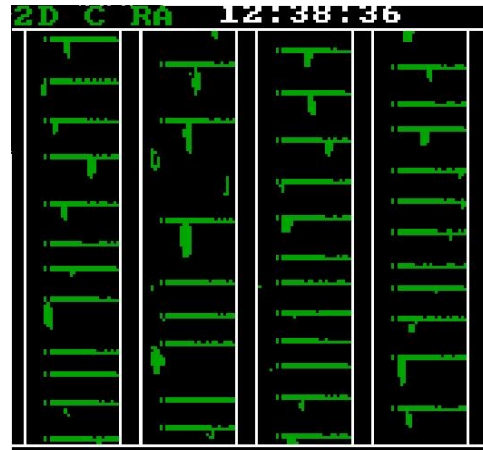


Fig. 11: OAP-2DC typical cloud element images near cloud top (above) and near cloud base (below). The horizontal scale of the single images is 750 µm (March 24th).

5. Summary

An artificial ice cloud of 2 m diameter, characterized by typical SLD parameters, has been produced by the Dornier 228 icing tanker permanently for more than 20 minutes duration. Visual cues on the following Dornier 328 test

aircraft were detected after a few minutes. SLD ice accretion on the wing leading edge upper surface, behind the pneumatic de-icing boots was characterized by a ridge-type shape. Artificial SLD ice of ridge-type shape on the full span of the upper wing surface degraded the maximum lift of the test aircraft by up to 50%. Visual cues for the pilot to detect SLD icing conditions and procedures for exiting them were introduced into the Do328-100 AFM. The artificial ice cloud provides SLD within the same diameter range as observed in natural supercooled clouds with about 10-20 times higher concentrations.

We have documented 2 cases of heavy aircraft icing with simultaneous documentation of cloud microphysical parameters. Our findings support the present picture of the cloud element spectra in mixed-phase clouds (e.g. Hobbs 1985, Politovitch, 1989; Rauber et al. 1991): separated into smaller cloud drops and huge (>200 μm sized) graupel crystals close to cloud base; more narrow spectra with temporarily >20 L^{-1} SLDs near cloud top. We further state:

SLD events do not seem to be too rare, since they were found during at least 2 of 5 flight missions. SLD occurrence was associated with simultaneously high LWC in the cloud drop mode ($\sim 20 \mu\text{m}$). On spatial scales of 10-20 km they carried a *significant*- but *not the main fraction* of soopercooled LWC (average over minutes). SLD-events leaving the FAR/JAR icing certification frame seem to occur as "peak events" on spatial scales of a few 100 m. The cloud top region is the preferable site for SLD-occurrence. (compare: Pobanz et al. 1994, Hobbs et al. 1985)

The most likely hazardous scenario for unexpectedly meeting SLD-conditions would be: Descent into the cloud top region of low-level stratiform cloud fields at temperatures close below -10°C . Repeated penetration of embedded convective cells - especially during extended holding patterns - could lead to irreversible ice accretion behind boot-protected regions. Such ice sockets may experience enhanced growth as soon as they expose extra surface to the free air stream. Even if the initial SLD-event is over, these extra surface could then collect small cloud drops which otherwise pass by the wing profile.

Acknowledgements

The authors would like to thank the flight test engineers, the technicians and the pilots from Dornier and DLR for their essential contribution to successful experiments in flying in difficult flight conditions. Contributions to this document by the following individuals are greatly appreciated by the authors: Gerhard Fuderer and Günther Halfmann from Dornier. The EURICE experiment was partly funded by the European Union.

References

- [1] Ashley, J. et al., 1995: FAA/Industry Meeting, June 21/22, 1995. Screening Airplanes for Susceptibility to SLD Roll Upset, ANM-160L, Los Angeles ACO
- [2] Cober, S.G., G.A. Isaac, and J.W. Strapp, 1995: Aircraft icing measurements in East Coast winter storms, *J. Appl. Meteor.*, 34, 88-100
- [3] Cober, G.C., J.W. Strapp, and G.A.- Isaac, 1996: An example of supercooled drizzle drops formed through a collision-coalescence process, *J. Appl. Meteor.*, 35, 2250-2260
- [4] Do328-100 Aircraft Flight Manual (AFM), Effectivity 23 Sept. 97, Dornier-Luftfahrt, D-82230 Wessling, Germany
- [5] Hauf, T. and F. Schröder, 1998 Supercooled Large Drops and Aircraft Icing. *Proceedings IWAIS Int. Conference, Reykjavik, 8-11 June, 1998*
- [6] Hauf, T., and F. Schröder, 1998: Observations of Aircraft Icing and Supercooled Large Drops, *Annales Geophysicae*, 16 Suppl2, C772, *Conference Contribution EGS 1998*,
- [7] Hauf, T., 1998: EURICE. WP2 Final Report, Deutsche Forschungsanstalt für Luft- und Raumfahrt (DLR) Oberpfaffenhofen Institut für Physik der Atmosphäre. (report available from EC Brussels)
- [8] Hobbs, P.V., and A. Rangno, 1985: Ice particle concentrations in clouds, *J. Atmos. Sci.*, 42, 2523-2549
- [9] Pobanz, B.M., J.D. Marwitz, and M.K. Politovich, 1994: Conditions associated with large drop regions, *J. Appl. Meteor.*, 33, 1366-1372
- [10] Politovitch, M.K. 1989: Aircraft icing caused by large supercooled droplets. *J. Appl. Meteor.*, 28, 856-868
- [11] Rauber, M.R. and A. Tokay, 1991: An explanation for the existence of supercooled water at the top of cold clouds, *J. Atmos. Sciences*, Vol.4, 1005-1023
- [12] Sand, W.R., W.A. Cooper, M.K. Politovich, and D.L. Veal, 1984: Icing conditions encountered by a research aircraft, *J. Climate Appl. Meteor.*, 23, 1427-1440
- [13] Strapp, J.W., R.A. Stuart, and G.A. Isaac, 1996: A Canadian climatology of freezing precipitation, and a detailed study using data from St. John's Newfoundland. *Proceedings FAA Int. Conference on Aircraft Inflight Icing*, Springfield, VA, FAA.